Available online at http://scik.org
J. Math. Comput. Sci. 10 (2020), No. 2, 316-338
https://doi.org/10.28919/jmcs/4376
ISSN: 1927-5307

ANALYSIS OF SEEPAGE PRESSURE IN DUAL-POROSITY RESERVOIR UNDER ELASTIC BOUNDARY

S.C. LI[1], M. ZHOU[1,*], P.S. ZHENG[1], X.X. DONG[1], Q.M. GUI[2]

[1]Institute of Applied Mathematics of XiHua University, Chengdu, Sichuan 610039, China

[2]Beijing Dongrunke Petroleum Technology Co., Ltd., Beijing 100029, China

Copyright © 2020 the author(s). This is an open access article distributed under the Creative Commons Attribution License, which permits unrestricted use, distribution, and reproduction in any medium, provided the original work is properly cited.

Abstract. In view of the large limitations of the dual-porosity media seepage model established in the early study, the elastic external boundary condition is newly presented in this paper, which can treats the idealized assumption (external boundary constant pressure, closed, infinite) in traditional model as a special case. Based on it, with considering the influence of well-bore storage, skin factors and external boundary radius on reservoir, an unstable seepage model under the elastic boundary is established first. then, the Laplace space solution of seepage model is obtained by using Laplace transform and similar structure theory in turn. Subsequently, by using Stehfest inversion transformation and the corresponding mapping software, the type curves are drawn, and the impacts of the main parameters on them are analyzed. The results indicate that the elastic coefficient has negative affect on the asymptotic rate of the type curve; And the type curves determined by different external boundary radii deviate during the later period of flow; Further more, the elastic coefficient affects the migration trajectory of the curves. Numerical simulation further verifies the scientificalness of introducing elastic external boundary conditions. The model established in this paper and the corresponding data analysis provide a more solid theoretical basis for the scientific analysis of the influence of reservoir parameters on reservoir pressure, and provide a new idea for the design and improvement of related well testing software.

Keywords: seepage model; dual-porosity media; similar structure theory; elasticity.

2010 AMS Subject Classification: 03F50.

*Corresponding author

E-mail address: zhouminmath@163.com

Received November 17, 2019

1. INTRODUCTION

The reservoir parameters are reversely calculated after matching actual theoretical curve to measured pressure curve by using modern well test analysis methods usually. Looking back to the research results obtained via modern well test analysis methods, we get obviously that though theoretical pressure type curve is similar to the actual measured, there are large errors with the theoretical [1], which brings about the error of the obtained reservoir parameters inevitably. How can we reduce such errors?In engineering, in addition to the instrumental measurement errors, the sources of error are mostly the over-idealized assumptions [2, 3]. The existing well test interpretation models are also based on specific idealized assumptions, including the ideal external boundary condition(closure, infinity and constant pressure)assumption. Based on this consideration, the authors contemplate a new external boundary condition (elastic external boundary) to decrease the errors of the obtained reservoir parameters.

What is the elastic outer boundary? In fact, the concept of elasticity has been widely used in economics, physics and engineering theory [4, 5, 6]. Alfred.Marshall, a famous economist, put forward the concept of elasticity: elasticity means the intensity or sensitivity of the relative change of dependent variables to the relative changes of independent variables. In 2010, Arthru P. Boresi (USA) published the ”Elastic Theory” in Engineering Mechanics which describes the application of elasticity in the branches of mechanics. The significance of putting forward the concept of elasticity is that elasticity solves the rigidity problem to a great extent in engineering problems. Hence, in this paper, with the help of the definition of elasticity itself, the elastic function and the elastic external boundary condition will be defined in the seepage problem, which will transform three kinds of ”rigid” external boundary conditions (closed, constant pressure, infinity) considered in the earlier studies into the elastic external boundary condition. Strictly to say, the elastic external boundary condition defined not only contains the three special boundary conditions but also extends the ideal outer boundary further, that makes it possible to reduce the error between theoretical pressure curve and the measured.

This paper focuses on the problem of dual-porosity media reservoirs. The research on dual-porosity media reservoirs originated in 1960, Barenblatt, Zheltov and Kochina proposed the

basic concept of fluid motion in fractured rock and based on some special hypothesis, the general equation of fluid flow [7] in dual-porosity media was obtained. In1997, E.S. Choi [8], M. Preshoand S. Wo, V. Ginting [9, 10] et al. established a seepage model under infinite, constant pressure and closed external boundary conditions for the problem of dual-porosity media and dual-permeability reservoir.Although the analytical solution was not given, the boundary conditions considered by the model had always been used by contemporary reservoir researchers, so the work done by the author is still meaningful. On the basis described above, Li Shunchu, Zheng Pengshe, Chen Liya et al. [11, 12, 13, 14] put forward the similar structure method and introduced the concept of similar kernel function after the deep study of the bottom hole pressure solution in dual-porosity media reservoir. And the solution of the model under three kinds of outer boundary conditions in theirs can be expressed as the form of continued fractions, which simplified and beautified the solution of the model. Shortly thereafter, The reservoir models of dual porosity medium reservoir under three kinds of external boundary conditions (closed, constant pressure, infinite) are established by Li Shunxhu, Xu Li, Xia Wenwen et al. [15, 16, 17]. After making use of the similar structure method and Stehfest numerical inversion method, a similar structure algorithm is developed to calculate well-bore pressure and pressure derivative of reservoir percolation model, and the type curves are drawn and analyzed at last, which provides a new idea for the design of the corresponding well test software.

On the basis of the above-mentioned analysis, in this paper, the elastic outer boundary condition will be introduced firstly when solving the mathematical model of unstable double porosity permeable flow, taking the three kinds of external boundary conditions (closure, infinity and constant pressure) considered in the past as special cases. Second, the similar construction method is used to solve the seepage model solution, and the numerical inversion method is used to draw the characteristic curve of bottom hole pressure in real space. But more than those, the influence of characteristic parameters under elastic boundary condition on the characteristics of unstable seepage pressure is analyzed, so as to make a more scientific guidance for the actual situation of oil and gas reservoir in reservoir development.

2. PRELIMINARIES

This paper is based on the following assumptions.

(1) Consider the shape of the matrix block to be a spherical block.

(2) The flow of a fluid is isothermal.

(3) There is no direct fluid flow between the pores and the well, and the flow sequence is:pore $\rightarrow$ crack $\rightarrow$ well.

(4) Fluid flow in the seepage field obeys Darcy's law.

(5) Do not take the influence of gravity into account.

(6) Only one well to produce.

(7) Inertia force is negligible.

The necessary symbols are as follows

Letter	Physical quantity	Company
P_i	Fluid pressure in real space	MPa
P_{iD}	Dimensionless fluid pressure in real space	dimensionless
$\overline{P}_{iD}$	Dimensionless fluid pressure in Laplace space	dimensionless
r_w	Well-bore radius	m
r	Distance from point to well-bore	m
r_D	Dimensionless distance from point to well-bore	dimensionless
R	Outer boundary radius	m
R_D	Dimensionless outer boundary radius	dimensionless
k_i	Permeability in a fractured system	mD
λ	Tandem flow coefficient	dimensionless
h	Reservoir thickness	m
ω	Storage ratio	dimensionless
Q	Surface production of wells	m^3/d
B	Volume coefficient of crude oil	dimensionless
C	Wellbore reservoir coefficient	m^3/MPa
ϕ_1	Porosity in fracture system	dimensionless
ϕ_2	Porosity in matrix system	dimensionless
μ	fluid viscosity	$mPa \cdot s$

Note: i=1, 2, w, respectively represent fracture system, matrix system, bottom hole.

2.1 Elasticity in seepage problem. In the process of fluid seepage, the pressure, affected by time and space, can be expressed as $p = p(x_1, x_2, x_3, t)$, so as to give the pressure drop expression $P = p_0 - p(x_1, x_2, x_3, t)$, where p_0 is the original formation pressure. In particular, the pressure drop expressed as $P = P(r,t) = p_0 - p(r,t)$ is considered to be a function of time and radial radius in the plane radial flow process.

In solving the issue of unstable seepage pressure dynamics, the state at every moment of the unstable seepage process can be considered stable. This method is referred to as the steady state replacement method [18]. Therefore, when defining the concept of elasticity below, the pressure drop can be considered as a function $P(r)$related only to the radial radius.

Definition 1:the pressure drop $P(r)$, a function of the fluid for radial radius r, is differentiable during seepage, then we call ε_r^P is the elastic function of $P(r)$ on r if $\varepsilon_r^P = \varepsilon_r^P(r) = -\frac{r}{P} \cdot \frac{\partial P}{\partial r} = -\frac{\partial lnP}{\partial lnr}$, and the value of ε_r^P at the point r_0 is the elastic coefficient of ε_r^P at point r_0, recorded as $\varepsilon_{r_0}^P$.

ε_r^P reflects the relationship between the relative rate of change of the radial radius and the relative rate of change of the pressure drop, also known as the sensitivity of P to r. For instance, the value of elastic function (elastic coefficient) is $\varepsilon_r^P(r_1)$ when $r = r_1$ at a certain time , Then the pressure drop is also approximately changed $\varepsilon_r^P(r_1)\%$ if the radial radius changes 1%.

2.2 Elastic external Boundary in the seepage problem of dual-porosity media. In this paper, we only need to establish the elastic function of the pressure drop $P_1(r)$ related to the radial radius r in the fracture system in view that fluid flows into the well-bore only through fractures in the process of formation seepage of dual-porosity media.

Let the external boundary $\Gamma : r = R$, according to the definition of elastic coefficient, the elastic coefficient of its boundary can be described as

$$\varepsilon_\Gamma^{P_1} = \varepsilon_R^{P_1} = -\frac{\partial lnP_1}{\partial lnr}|_{r=R} \tag{2.2.1}$$

Three kinds of external boundary conditions (closed, constant pressure, infinite) are considered in the study of early petroleum engineering as follows.

(1) The equation $\frac{\partial P_1}{\partial r}|_{r=R}=0$ is established when the outer boundary is closed, and we get $\varepsilon_\Gamma^{P_1}=0$ at this time.

(2) The equation $P_1|_{r=R}=0$ is established when the outer boundary pressure is constant and we get $\varepsilon_\Gamma^{P_1}\to+\infty$ at this time.

(3) The equation $P_1|_{r\to+\infty}=0$ is established when the outer boundary is infinite and we get $R\to+\infty$ at this time.

Therefore the following definition can be given.

Definition 2: Let the pressure drop of the fracture system be $P(r)$ as a function of the radial radius r and the outer boundary radius is R, then

$$[\varepsilon_\Gamma^{P_1}P_1+r\frac{\partial P_1}{\partial r}]_{r=R}=0 \tag{2.2.2}$$

is called the elastic outer boundary condition of the fluid.

3. MAIN RESULTS

3.1 basic assumptions and mathematical models. Combined with the initial condition and boundary condition, the seepage model of dual-porosity medium can be established as follows [19, 20, 21]

$$\begin{cases}
\frac{\partial^2 P_1}{\partial r^2}+\frac{1}{r}\frac{\partial P_1}{\partial r}-\frac{\mu}{k_1}q=\frac{\phi_1 c_1\mu}{k_1}\frac{\partial P_1}{\partial t}\\
\frac{\partial^2 P_2}{\partial r^2}+\frac{2}{r}\frac{\partial P_2}{\partial r}=\frac{\phi_2 c_2\mu}{k_2}\frac{\partial P_2}{\partial t}\\
\frac{\partial P_2}{\partial r}|_{r=0}=0\\
P_2(r,t)|_{r=r_1}=P_1\\
q=\frac{3}{r_1}\frac{k_2}{\mu}\frac{\partial P_2}{\partial r}|_{r=r_1}\\
P_1(r,0)=P_2(r,0)=0\\
P_w(t)=[P_1-Sr\frac{\partial P_1}{\partial r}]|_{r=r_w}\\
r\frac{\partial P_1}{\partial r}|_{r=r_w}=\frac{141.2\mu}{k_1 h}[-BQ+C\frac{dP_1}{dt}]\\
(\varepsilon_\Gamma^{P_1}P_1+r\frac{\partial P_1}{\partial r})_{r=R}=0\text{(the external boundry condition)}
\end{cases} \tag{3.1.1}$$

3.2 Transformation and solution of the model.

3.2.1 Dimensional seepage model of matrix system under elastic boundary. To facilitate the solution, the following dimensionless quantities are introduced.

$$\begin{cases} r_{2D} = \frac{r}{r_1}, P_{iD} = \frac{k_1 h}{141.2BQ\mu} P_i (i = 1,2) \\ C_D = \frac{C}{1.191(\phi_1 c_1 + \phi_2 c_2) h r_w^2} \\ t_D = \frac{2.637\times 10^{-4}}{(\phi_1 c_1 + \phi_2 c_2)\mu r_w^2} k_1 t \\ \omega = \frac{\phi_1 c_1}{\phi_1 c_1 + \phi_2 c_2}, \lambda = 15(\frac{r_w}{r_1})\frac{k_2}{k_1} \end{cases}$$

Based on the assumption of 3.1.1, the dimensionless seepage model of matrix system is obtained by dimensionless treatment of the variables in the seepage model of matrix system.

$$\begin{cases} \frac{\partial^2 P_{2D}}{\partial r_{2D}^2} + \frac{2}{r_{2D}} \frac{\partial P_{2D}}{\partial r_{2D}} = \frac{3.9555\times 10^3 (1-\omega)}{\lambda} \frac{\partial P_{2D}}{\partial t_D} \\ P_{2D}(r_{2D}, t_D)|_{r_{2D}=1} = P_{1D} \\ \frac{\partial P_2}{\partial r} = 0 \\ P_2(r,t)|_{r=r_1} = P_2 \end{cases} \tag{3.2.1}$$

For (3.2.1), taking the Laplace transform as follows on dimensionless time t_D.

$$\overline{P_{2D}} = \int_0^\infty e^{-zt_D} P_{2D} dt_D$$

Where z is a parameter, and then we get

$$\begin{cases} \frac{d^2 \overline{P_{2D}}}{dr_{2D}^2} + \frac{2}{r_{2D}} \frac{d\overline{P_{2D}}}{dr_{2D}} = W^2 \overline{P_{2D}} \\ \overline{P_{2D}}(r_{2D}, z)|_{r_{2D}=1} = \overline{P_{1D}} \\ \frac{\overline{dP_{2D}}}{dr_{2D}} = 0 \end{cases} \tag{3.2.2}$$

Where $W = \frac{3.9555\times 10^3 (1-\omega) z}{\lambda}$.Its easy to obtained the answer(derivation details are included in Appendix A)

$$\frac{\overline{dP_{2D}}}{dr_{2D}}|_{r_{2D}=1} = (W\coth(W) - 1)\overline{P_{1D}} \tag{3.2.3}$$

3.2.2 Dimensional seepage model of fracture system under elastic boundary. On the basis of section 3.2.1, the following dimensionless quantities are introduced.

$$\begin{cases} r_{1D} = \frac{r}{r_w}, R_{1D} = \frac{R}{r_w} \\ P_{wD} = \frac{k_1 h}{141.2BQ\mu} P_w \end{cases}$$

The dimensionless mathematical model of fluid seepage in fracture system is obtained as follows.

$$\begin{cases} \frac{\partial^2 P_{1D}}{\partial r_{1D}^2} + \frac{1}{r_{1D}} \frac{\partial P_{1D}}{\partial r_{1D}} - \frac{\lambda}{5}(W\coth(W)-1)P_{1D} = 2.637\times 10^{-4}\omega \frac{\partial P_{1D}}{\partial t_D} \\ P_{wD} = [P_{1D} - Sr_{1D}\frac{\partial P_{1D}}{\partial r_{1D}}]|_{r_{1D}=1} \\ (C_D \frac{\partial P_{wD}}{\partial t_D} - r_{1D}\frac{\partial P_{1D}}{\partial r_{1D}})|_{r_{1D}=1} = 1 \\ (\varepsilon_\Gamma^{P_{1D}} P_{1D} + R_D \frac{\partial P_{1D}}{\partial r_{1D}})_{r_{1D}=R_D} = 0 \end{cases} \tag{3.2.4}$$

For (3.2.4), the Laplace transformation for dimensionless time t_D is obtained

$$\begin{cases} \frac{d^2\overline{P_{1D}}}{dr_{1D}^2} + \frac{1}{r_{1D}}\frac{d\overline{P_{1D}}}{dr_{1D}} = [\frac{\lambda}{5}(W\coth(W)-1) + 2.637\times 10^{-4}\omega z]\overline{P_{1D}} \\ \overline{P_{wD}} = [\overline{P_{1D}} - Sr_{1D}\frac{d\overline{P_{1D}}}{Dr_{1D}}]|_{r_{1D}=1} \\ (C_D z\overline{P_{wD}} - r_{1D}\frac{d\overline{P_{1D}}}{dr_{1D}})|_{r_{1D}=1} = \frac{1}{z} \\ (\varepsilon_\Gamma^{P_{1D}}\overline{P_{1D}} + R_D\frac{d\overline{P_{1D}}}{dr_{1D}})_{r_{1D}=R_D} = 0 \end{cases} \tag{3.2.5}$$

Then assuming $f(z) = \omega + \frac{\lambda}{5z}(W\coth(W)-1)$, (3.2.5) could be simplified as follows.

$$\begin{cases} \frac{d^2\overline{P_{1D}}}{dr_{1D}^2} + \frac{1}{r_{1D}}\frac{d\overline{P_{1D}}}{dr_{1D}} - zf(z)\overline{P_{1D}} = 0 \\ (-kC_D z\overline{P_{1D}} + (1+kC_D zS)\frac{d\overline{P_{1D}}}{dr_{1D}})|_{r_{1D}=1} = \frac{1}{z} \\ (\varepsilon_\Gamma^{P_{1D}}\overline{P_{1D}} + R_D\frac{d\overline{P_{1D}}}{dr_{1D}})_{r_{1D}=R_D} = 0 \end{cases} \tag{3.2.6}$$

where $k = 141.2\times 1.191\times 2.637\times 10^{-4}$.

3.2.3 Similarity Construction Theory for Boundary value problems of differential equations. Theorem 1: In the form of

$$\begin{cases} y'' + \frac{1}{x}y' - Ay = 0, x > 0 \\ y'|_{x=a} = -1 \\ (Ey + Fy')_{x=b} = 0 \end{cases} \tag{3.2.8}$$

this boundary value problem of ordinary differential systems have the following form of solution where a, b, A, E, F are the real constant and $A > 0, E^2 + F^2 \neq 0, 0 < a < b$:

$$y = \Phi(x) = \frac{1}{\sqrt{A}} \frac{E\varphi_{0,0}(x,b,\sqrt{A}) + F\sqrt{A}\varphi_{0,1}(x,b,\sqrt{A})}{E\varphi_{1,0}(a,b,\sqrt{A}) + F\sqrt{A}\varphi_{1,1}(a,b,\sqrt{A})} \tag{3.2.9}$$

here

$$\varphi_{m,n}(x,y,z) = K_m(xz)I_n(yz) + (-1)^{m-n+1}I_m(xz)K_n(yz) \tag{3.2.10}$$

Where $K_l(\bullet), I_l(\bullet)$ are the first and second order variant Bessel functions respectively (derivation details are included in Appendix B).

In order to solve the problem of definite solution (3.2.7), it is necessary to further improve the formula (3.2.8) and generalize the boundary conditions $x = a$. For this reason, the following theorem is given.

Theorem 2: In the form of

$$\begin{cases} y'' + \frac{1}{x}y' - Ay = 0, x > 0 \\ [By + (1 + BC)y']|_{x=a} = D \\ (Ey + Fy')_{x=b} = 0 \end{cases} \tag{3.2.11}$$

this boundary value problem of ordinary differential systems have the following form of solution where a, b, A, B, C, D, E, F are the real constant and $A > 0, E^2 + F^2 \neq 0, 0 < a < b$ (derivation details are included in Appendix C):

$$y = D \cdot \frac{1}{B + \frac{1}{C - \Phi(a)}} \cdot \frac{1}{C - \Phi(a)} \cdot (-\Phi(x)) \tag{3.2.12}$$

In fact, $\Phi(x)$ in (3.2.9) can be considered as a similar kernel function of the boundary value problem (3.2.11), and (3.2.12) is a similar structural formula of the solution of the boundary value problem (3.2.10). Therefore, in order to obtain the solution of the boundary value problem

(3.2.11), it can be completed according to the similar structure method [13]. The method steps are as follows:

Step1:The function is constructed from the parameter A and the independent variable x in the solution equation and its value a,b on the boundary are as follows:

$$\varphi_{0,0}(x,b,\sqrt{A}),\varphi_{0,1}(x,b,\sqrt{A}),\varphi_{1,0}(x,b,\sqrt{A}),\varphi_{1,1}(x,b,\sqrt{A})$$

then calculate the value of $\varphi_{1,0}(a,b,\sqrt{A})$ and $\varphi_{1,1}(a,b,\sqrt{A})$

Step2:From the constant E,F of the boundary condition $(Ey+Fy^{'})_{x=b}=0$, according to the formula (3.2.8) too, a similar kernel function$\Phi(x)$ is obtained and the value $\Phi(a)$ is calculated.

Step3:From the constants B,C,D in the boundary condition $[By+(1+BC)y^{'}]|_{x=a}=D$ at $x=a$ in (3.2.10), according to the formula (3.2.11) too, the solution of the boundary value problem (3.2.10) is obtained.

3.3 Solution of Seepage Model. By comparing the boundary value problems (3.2.7) and (3.2.11), it is not difficult to find that the two boundary value problems are consistent when the parameters and variables are replaced by table 1.

Therefore, a similar kernel function, which is easy to obtain the solution of the (3.2.6) model, is as follows.

$$\Phi(r_{1D})=\frac{\varepsilon_{\Gamma}^{P_{1D}}\varphi_{0,0}(r_{1D},R_D,\sqrt{zf(z)})+R_D\sqrt{zf(z)}\varphi_{0,1}(r_{1D},R_D,\sqrt{zf(z)})}{\sqrt{zf(z)}[\varepsilon_{\Gamma}^{P_{1D}}\varphi_{1,0}(1,R_D,\sqrt{zf(z)})+R_D\sqrt{zf(z)}\varphi_{1,1}(1,R_D,\sqrt{zf(z)})]} \tag{3.3.1}$$

and the Laplace space solution of dimensionless pressure of the crack system can be obtained as follows .

$$\overline{P_{1D}}(r_{1D},z)=\frac{1}{z}\cdot\frac{1}{kC_Dz+\frac{1}{S+\Phi(1)}}\cdot\frac{1}{S+\Phi(1)}\cdot(-\Phi(r_{1D})) \tag{3.3.2}$$

Owing to $\overline{P_{wD}}=[\overline{P_{1D}}-Sr_{1D}\frac{d\overline{P_{1D}}}{dr_{1D}}]|_{r_{1D}=1}$, the Laplace space solution of dimensionless bottom-hole pressure can be obtained as follows.

$$\overline{P_{wD}}=\frac{1}{z}\cdot\frac{1}{kC_Dz+\frac{1}{S+\Phi(1)}} \tag{3.3.3}$$

TABLE 1. Parameter and variable replacement table

Parameters and variables in Boundary value problem (3.2.11)	Parameters and variables in Boundary value problem (3.2.7)
x	r_{1D}
y	$\overline{P_{1D}}$
a	1
b	R_D
A	$zf(z)$
B	$-kC_Dz$
C	$-S$
D	$\frac{1}{z}$
E	$\varepsilon_{\Gamma}^{P_{1D}}$
F	R_D

4. SENSITIVITY ANALYSIS

By using Stehfest numerical inversion method, the Laplace space solution of dimensionless bottom hole pressure is inversed into real space. Through the numerical simulation of the mapping software and the analysis of the influence of typical parameters on the bottom hole pressure and pressure derivative under the elastic outer boundary, the law of the bottom hole pressure and pressure derivative changes with time under the elastic boundary is obtained finally.

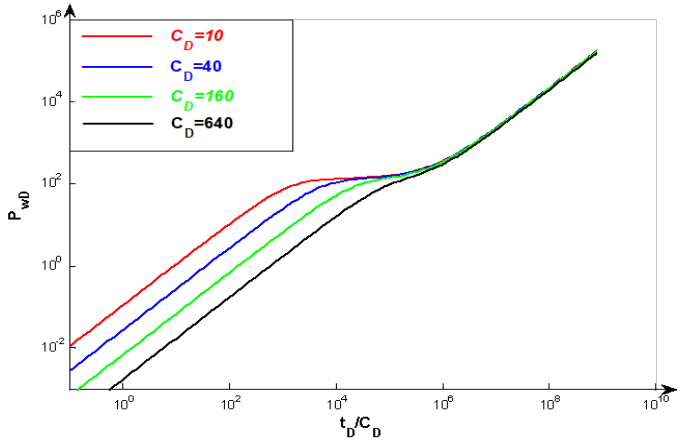

FIGURE 1. Effect of C_D for the type curves

4.1 Effect of $\varepsilon_{\Gamma}^{P_{1D}}$ and C_D for the type curves. Fig.1 shows the variation of dimensionless bottom hole pressure with time under the action of well-bore reservoir C_D. The figure firstly shows that the well-bore reservoir mainly affects the initial stage of fluid flow.Secondly, the larger the well-bore reservoir is, the smaller the dimensionless bottom hole pressure well be. Thirdly, the dimensionless bottom hole pressure increases at a relatively stable rate for a period of time. When the matrix system fluid flows to the fracture system, the growth rate of the curve appears to be transiently stable, and then continues to increase. The characteristic curve determined by different well-bore reservoir coefficients eventually asymptotically follows a curve.

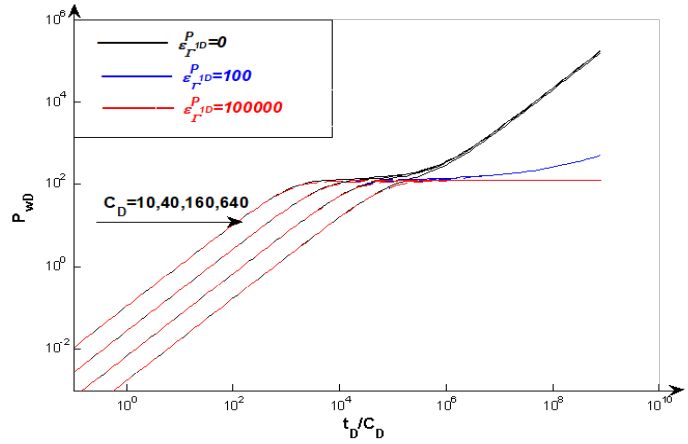

FIGURE 2. Effect of $\varepsilon_{\Gamma}^{P_{1D}}$ and C_D for the type curves

Fig.2 shows the variation of dimensionless bottom hole pressure with time under the interaction of elastic boundary and well-bore reservoir. It is easy to see from the figure that in the initial stage of mining, the curves with the same coefficient of elasticity for different well-bore reservoirs almost coincide. At this time, well-bore reservoir is the main influencing factor of dimensionless bottom-hole pressure. When the characteristic curve shows asymptotic phenomenon, the elastic boundary becomes the main factor affecting the curve; the elastic coefficient is positively correlated with the inclination rate of the asymptotic curve, that is, the larger the elastic coefficient is , the faster the dimensionless bottom hole pressure increase rate will be.

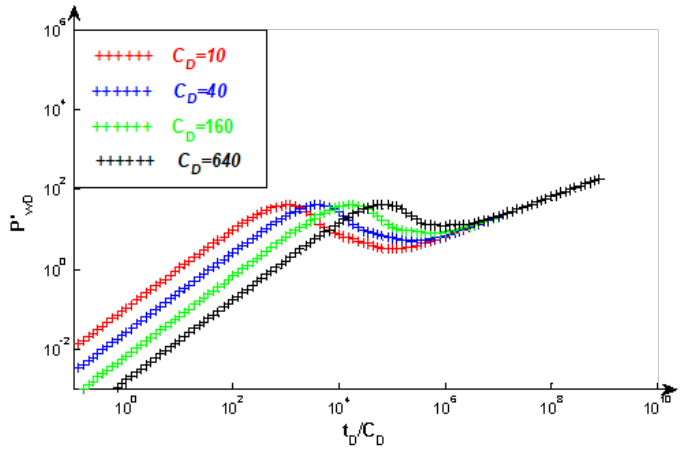

FIGURE 3. Effect of C_D for the type curves

Fig.3 shows the effect of well-bore reservoir on dimensionless bottom-hole pressure derivative. It can be seen from the figure that the dimensionless pressure derivative increases continuously in the initial stage of production. When the matrix system fluid flows to the fracture system, the dimensionless pressure derivative becomes smaller in a short time and then continues to increase, and finally characteristic curve is asymptotic to a curve. The value of the well-bore storage coefficient is positively correlated with the time it takes for the peak to appear, that is, the smaller the C_D, the earlier the peak appears.

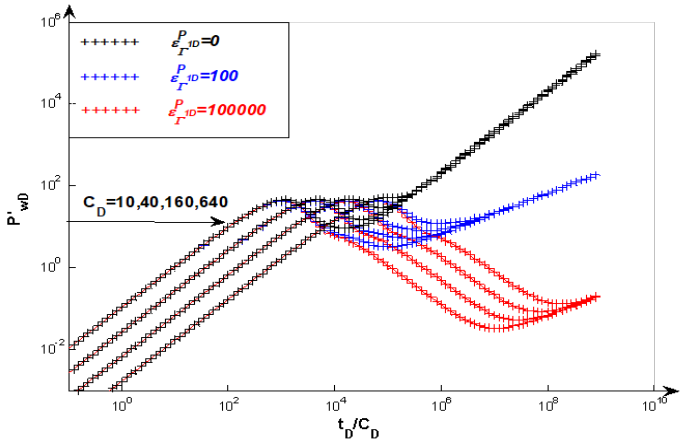

FIGURE 4. Effect of $\varepsilon_{\Gamma}^{P_{1D}}$ and C_D for the type curves

Fig.4 shows the variation of dimensionless bottom derivative with time under the interaction of elastic boundary and well-bore reservoir. It can be seen from the diagram that at the beginning of production, although the elastic outer boundary has little effect on the dimensionless pressure derivative of well-bore reservoir, the smaller the C_D value, the greater the bottom-hole pressure of dimensionless hole. The characteristic curve has peaks and wave troughs, and after the peak appears, the elastic boundary plays a leading role. The elastic coefficient is inversely related to the dimensionless pressure derivative at the trough and positively correlated with the asymptotic time of the curve.

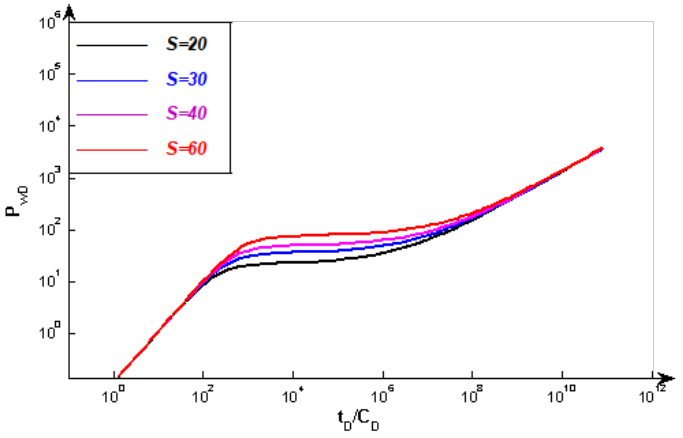

FIGURE 5. Effect of S for the type curves

4.2 Effect of $\varepsilon_{\Gamma}^{P_{1D}}$ and S for the type curves. **Fig.5** shows the variation of dimensionless bottom hole pressure with time under the action of epidermal factor S. It can be seen from the diagram that the characteristic curves determined by different epidermal factors are significantly different in the middle period of fluid flow, and the epidermal factors are positively correlated with the dimensionless bottom hole pressure, and in the early and late stages, the characteristic curves are asymptotically at a certain curve at a relatively stable rate.

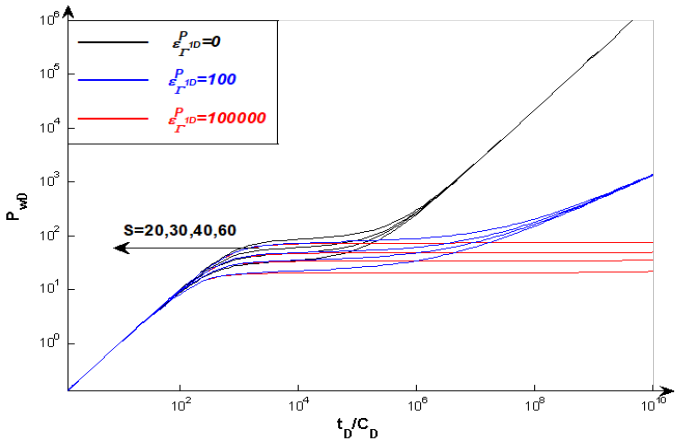

FIGURE 6. Effect of $\varepsilon_{\Gamma}^{P_{1D}}$ and S for the type curves

Fig.6 shows the variation law of the pressure of the dimensionless well bottom over time under the interaction of elastic boundary and skin factor. As can be seen from the figure , the characteristic curve shows a remarkable difference after the pressure of the dimensionless well bottom is increased to a certain value at a relatively stable speed, and the characteristic curve of the same elastic coefficient is asymptotic to a curve after a period of relative stable period. The elastic coefficient is negatively correlated with the asymptotic velocity and positively correlated with the pressure derivative at the asymptotic point.

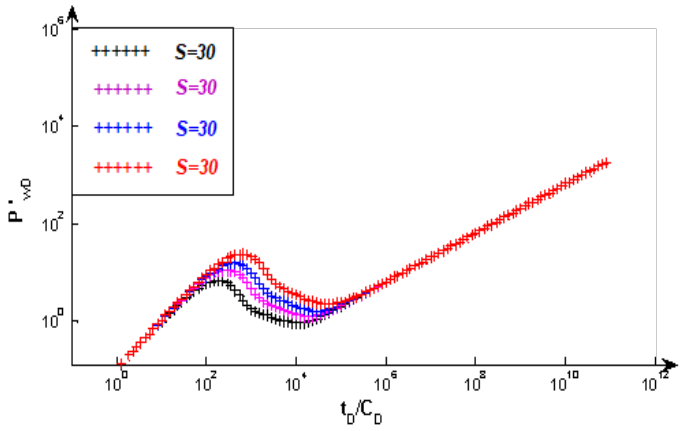

FIGURE 7. Effect of S for the type curves

Fig.7 shows the variation of dimensionless pressure derivatives over time under the influence of epidermis effect. It can be seen from the diagram that the overall change of the characteristic curve is hump, the dimensionless pressure derivative is positively correlated with the epidermal factor in the middle period of fluid flow, and the characteristic curve is finally asymptotically in a curve.

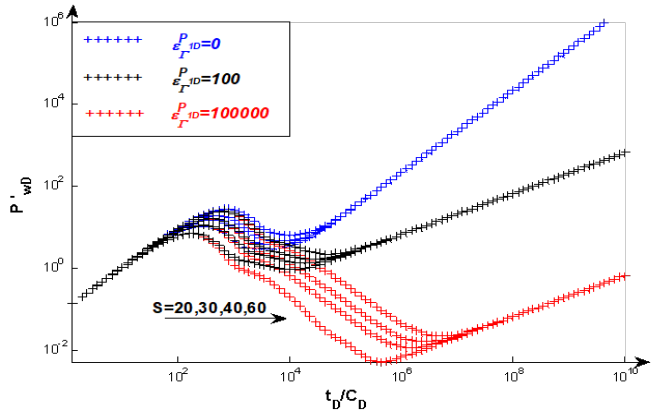

FIGURE 8. Effect of $\varepsilon_{\Gamma}^{P_{1D}}$ and S for the type curves

Fig.8 shows the variation of the dimensionless bottom-hole pressure derivative over time with the elastic boundary and the skin factor. It can be seen from the figure that the characteristic curve with the same elastic coefficient is finally asymptotic to a curve. The characteristic curves determined by different skin factors are different. The total length of the segments is different.

The elastic coefficient is positively correlated with the total length of the significant difference, negatively correlated with the asymptotic velocity of the curve, and negatively correlated with the pressure derivative when the curve is asymptotic.

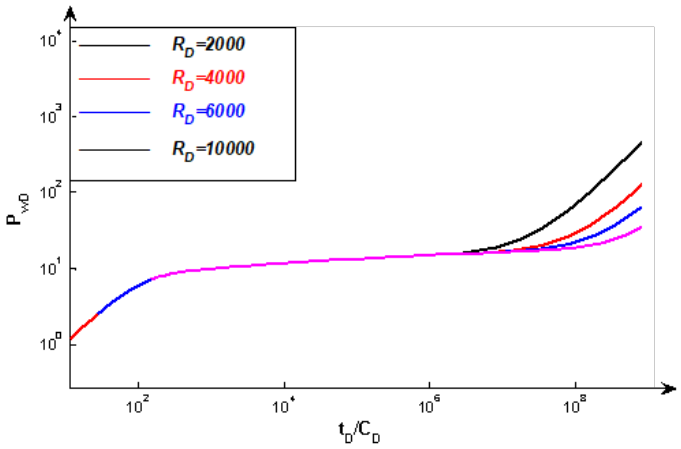

FIGURE 9. Effect of R_D for the type curves

4.3 Effect of $\varepsilon_\Gamma^{P_{1D}}$ and R_D for the type curves. Fig.9 shows the variation of the dimensionless bottom hole pressure over time under the outer boundary radius. It can be seen from the figure that the outer boundary radius mainly affects the late stage of fluid flow; at the same time, the smaller the dimensionless bottom hole pressure is with the larger the outer boundary radius.

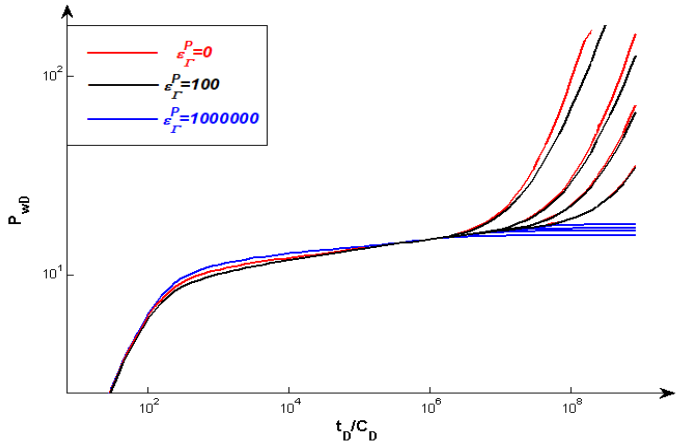

FIGURE 10. Effect of $\varepsilon_\Gamma^{P_{1D}}$ and R_D for the type curves

Fig.10 shows the variation of the dimensionless bottom hole pressure over time under the interaction of the elastic boundary and the outer boundary radius. It can be seen from the figure

that the elastic outer boundary condition does not affect the overall trend of the characteristic curve determined by R_D. characteristic curve in the later stage of flow appears to be offset. When the outer boundary radius is the same, the larger the inclination of the characteristic curve is with the larger the elastic coefficient.

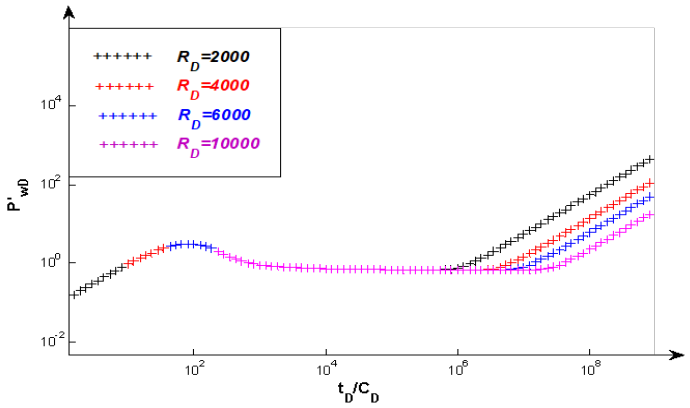

FIGURE 11. Effect of R_D for the type curves

Fig.11 shows the variation of dimensionless bottom-hole pressure derivatives over time under the effect of R_D. It can be seen from the figure that the dimensionless pressure derivative increases briefly at the initial stage of flow and then decreases briefly. After a period of relative stability, the dimensionless pressure derivative continues to increase: the smaller the R_D, the earlier the characteristic curve deviates the steady state.

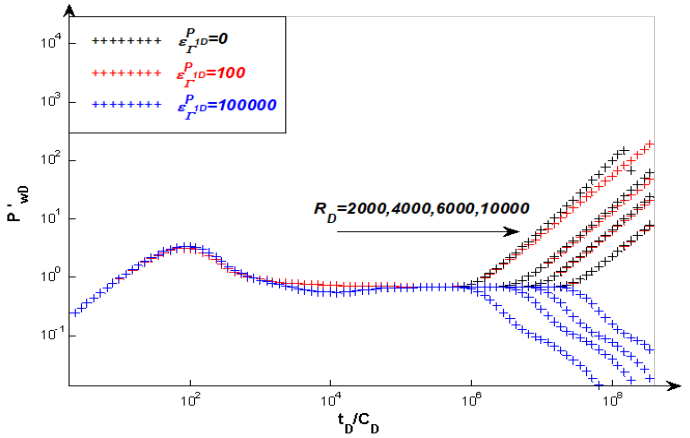

FIGURE 12. Effect of $\varepsilon_{\Gamma}^{P_{1D}}$ and R_D for the type curves

Fig.12 shows the variation of the dimensionless bottom hole pressure with time under the interaction of the elastic boundary and the outer boundary radius. It can be seen from the figure that different elastic boundaries and different outer boundary radii play different roles in the later stage of the flow; the difference of the elastic coefficients affects the offset trajectory of the curve, and does not affect the time when the characteristic curve appears to be offset.

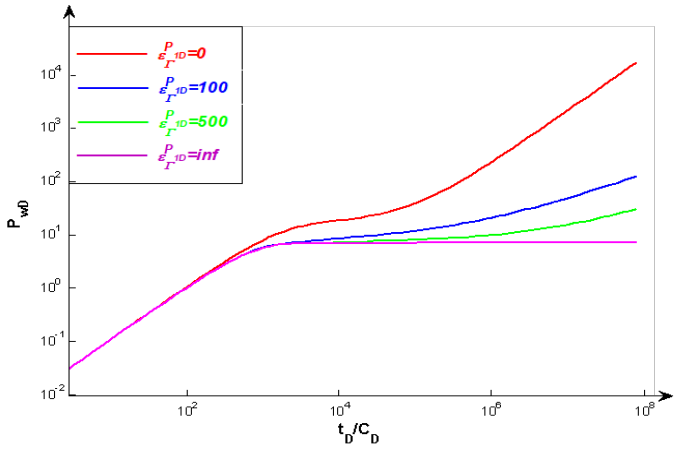

FIGURE 13. Effect of $\varepsilon_{\Gamma}^{P_{1D}}$ for the type curves

4.4 Effect of $\varepsilon_{\Gamma}^{P_{1D}}$ for the type curves. Fig.13 shows the influence of elastic boundary on dimensionless bottomhole pressure when other parameters are not changed. The curve shows that the greater the elastic coefficient, the more gentle the pressure change in the middle period of flow, that is, the greater the elastic coefficient is, the smaller the dimensionless bottom hole pressure is at the same time.

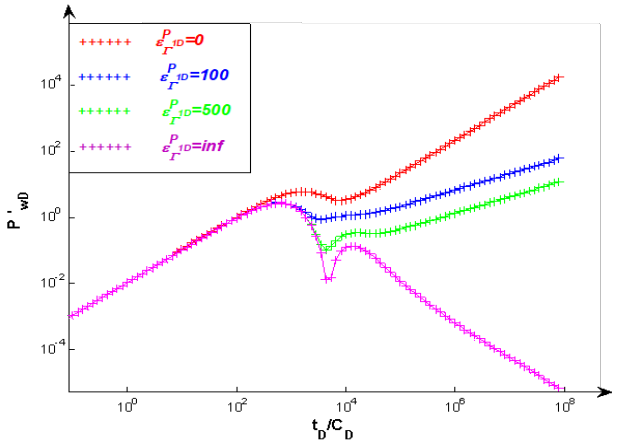

FIGURE 14. Effect of $\varepsilon_{\Gamma}^{P_{1D}}$ for the type curves

Fig.14 shows the effect of the elastic boundary on the dimensionless pressure derivative when other parameters are fixed. No matter what value the elastic coefficient takes, the curve falls between the curves determined by the elastic coefficient $\varepsilon_{\Gamma}^{P_{1D}} = 0$ and $\varepsilon_{\Gamma}^{P_{1D}} = inf$, which further verifies the scientificity of introducing the elastic outer boundary condition.

5 Conclusions

Considering the influence of well-bore storage, skin factors and external boundary radius on reservoir pressure, an unsteady seepage model under elastic boundary is established. The unsteady seepage systems in dual-porosity media is obtained by using Laplace transformation and initial boundary conditions. Using the similar construction theory, the expression of the dimensionless pressure solution of the matrix system and the fracture system under the elastic boundary is obtained.

In view of the limitation of the traditional model in describing the percolation law, the elastic coefficient and the elastic outer boundary conditions are defined based on the steady-state displacement method. The variation law of bottom hole pressure and pressure derivative is obtained through comprehensive analysis of well-bore reservoir, skin factor, outer boundary radius and elastic boundary. The research shows that under the wellbore reservoir effect, the characteristic curve will have extreme points. When the value of C_D is smaller, picture shows that the inflection point and extreme point appear earlier. The smaller the S value in the middle

phase of the flow is, the smaller the bottom hole pressure and pressure derivative in the same period. The smaller the R_D in the later stage of fluid flow, the earlier migration occurs in the characteristic curve. When the R_D is fixed, the elastic coefficient affects the asymptotic time of the characteristic curve. The larger the elastic coefficient, the longer the asymptotic time is. The greater the medium-term elastic coefficient, the more gradual the pressure changes. When C_D and S are fixed, the elastic coefficient affects the deviation of the curve steady state trajectory.

the elastic external boundary condition defined not simply take the external boundary conditions (closed, infinite and constant pressure) considered in the past are regarded as special cases but can solve more complex boundary seepage problem with taking difference elastic coefficient. Therefore, the introduction of elastic outer boundary makes it possible to reduce the error looking from the type curve between theoretical pressure curve and the measured. At the same time, the model and corresponding data analysis established in this paper provide a solid theoretical basis for the scientific analysis of the influence of reservoir coefficient on reservoir pressure, and provide a new idea for the design and improvement of the corresponding well testing software.

ACKNOWLEDGEMENT

The authors would like to thank the anonymous referees for their valuable comments and suggestions. this work is supported by the Education Natural Science Key Project of Si Chuan Provincial Department (NO: 15ZA0135), the first batch of science and technology projects of Si Chuan Science and Technology Department (basic research - key research) (NO: 2015JY0245) and innovation fund of Xihua University (NO: ycjj2018032).

CONFLICT OF INTERESTS

The author(s) declare that there is no conflict of interests.

REFERENCES

[1] Y.Y. Zhang, J. Yao, The mechanism and method of well test interpretation, China University of Petroleum Press. (2006), 67-79.

[2] H.J. Zou and L.Q. Wang, Comprehensive error analysis of elastodynamic equations, Chinese J. Mech. Eng. 27(2)(1991), 7-12.

[3] S.T. Liu, G.R. Pan, Monitoring the error sources and deformation analysis based on laser scanning tunnel deformation, J. Railway Eng. Soc. 30 (5)(2013), 69-74.

[4] M. Beltran, Marta. BECloud: A new approach to analyse elasticity enablers of cloud services. Future Gen. Computer Syst. 64(2016), 39-49.

[5] Isabella Schulte. Price and income elasticities of residential energy demand in germany. Social Science Electronic Publishing, (2016).

[6] Barthel, Anne Christine. Revisiting the role of elasticity in multiproduct monopoly pricing. Economics Letters 167(2018), 120-123.

[7] G. I Barenblatt, Iu. P Zheltov, and I. N Kochina. Basic concepts in the theory of seepage of homogeneous liquids in fissured rocks [strata]. J. Appl. Math. Mech. 24(5)(1960), 1286-1303.

[8] E.S. Choi, T. Cheema, and M. R. Islam. A new dual-porosity/dual-permeability model with non-darcian flow through fractures. J. Petroleum Sci. Eng. 17(3-4)(1997), 331-344.

[9] S. BrouyRe. Modelling the migration of contaminants through variably saturated dual-porosity, dual-permeability chalk. J. Contaminant Hydrol. 82(3)(2006), 195-219.

[10] M. Presho, S. Wo, and V. Ginting. Calibrated dual porosity, dual permeability modeling of fractured reservoirs. J. Petroleum Sci. Eng. 77(3)(2011), 326-337.

[11] J.D. Tian, S.C. Li . The Formal Similarity of Solutions in the Laplace Space on the Class of Quasilinear Partial Differential Equation System. Math. Theory Appl. 2004(2)(2004), 66-73.

[12] S. C. Li Z. C. Chen, P. H. Liu. Similar structure of solution for complex bessel equations. J. Chongqing Technol. Business Univ. (Nat. Sci. Ed.), 23(1)(2006), 1-4.

[13] W.B. Zhu P.S. Zheng, S.C. Li. Similar structure of pressure distribution in composite dual-porosity media reservoir. Drilling process, 31(4)(2008), 80-81.

[14] X. Lai L.Y. Chen, S.C. Li. Solution and analysis of bottom hole pressure in double-porous media composite reservoir. Drilling process, 33(5)(2010), 52-54 .

[15] X. T. Bao, S. C. Li, and D. D. Gui. Similar constructive method for solving the nonlinear spherical percolation model in dual-porosity media. Advanced Materials Research, 631-632(2013), 265-271.

[16] L. Xu, X. Liu, L. Liang, S. Li, and L. Zhou.The similar structure method for solving the model of fractal dual-porosity reservoir. Math. Probl. Eng. 2013(4)(2013), 1-9 .

[17] W. Xia, S. Li, and D. Gui. The similar structure method for solving the radial seepage model of fractal composite reservoir with double-porosity. Amer. J. Appl. Math. Stat. 3(2)(2015), 80-85.

[18] W. Zhu, Q.I. Qian, M.A. Qian, J. Deng, M. Yue, and Y. Liu. Unstable seepage modeling and pressure propagation of shale gas reservoirs. Petroleum Explor. Develop. 43(2)(2016), 285-292 .

[19] X.J. Kong. Higher seepage mechanics. China University of Science and Technology Press, (2010)

[20] A. Mehrabian, C. Liu and Y. Abousleiman, Poroelastic dual-porosity/dual-permeability after-closure pressure-curves analysis in hydraulic fracturing. SPE J. 22(01)(2017), 198-218.

[21] R. S. Nie, Y. F. Meng, Y. L. Jia, F. X. Zhang, X. T. Yang, and X. N. Niu. Dual porosity and dual permeability modeling of horizontal well in naturally fractured reservoir. Transport in Porous Media, 92(1)(2012), 213-235.